BRIEF COMMUNICATION

A novel technique of detecting MRI-negative lesion in focal symptomatic epilepsy: Intraoperative ShearWave Elastography

*†Huan Wee Chan, ‡Ronit Pressler, *Christopher Uff, §Roxanna Gunny, ‡Kelly St Piers, ¶Helen Cross, †Jeffrey Bamber, *Neil Dorward, #William Harkness, and #Aabir Chakraborty

Epilepsia, 55(4):e30–e33, 2014
doi: 10.1111/epi.12562

Mr. Huan Wee Chan is a clinical research fellow and a registrar in neurosurgery in London, United Kingdom.

Summary

Focal symptomatic epilepsy is the most common form of epilepsy that can often be cured with surgery. A small proportion of patients with focal symptomatic epilepsy do not have identifiable lesions on magnetic resonance imaging (MRI). The most common pathology in this group is type II focal cortical dysplasia (FCD), which is a subtype of malformative brain lesion associated with medication-resistant epilepsy. We present a patient with MRI-negative focal symptomatic epilepsy who underwent invasive electrode recordings. At the time of surgery, a novel ultrasound-based technique called ShearWave Elastography (SWE) was performed. A 0.5 cc lesion was demonstrated on SWE but was absent on B-mode ultrasound and 3-T MRI. Electroencephalography (EEG), positron emission tomography (PET), and magnetoencephalography (MEG) scans demonstrated an abnormality in the right frontal region. On the basis of this finding, a depth electrode was implanted into the lesion. Surgical resection and histology confirmed the lesion to be type IIb FCD.

KEY WORDS: Focal epilepsy, Elastography, Shear wave, Cortical dysplasia, Intraoperative ultrasound.

Focal symptomatic epilepsy is the most common type of epilepsy in humans and usually does not respond to medical therapy. Although a majority of these patients will have a demonstrable lesion on magnetic resonance imaging (MRI), a small proportion will have normal MRI appearance, that is, MRI-negative cases, where the surgical outcomes are not as favorable.[1] Because the surgical outcomes depend on completeness of resection of the epileptogenic focus,[2] to improve detection of the lesion we employed a novel technique of elasticity imaging, called ShearWave Elastography (SWE; SuperSonic Imagine, Aix-en-Provence, France). This is a noninvasive tissue elasticity imaging technique that maps tissue stiffness in real time. We hypothesize that the epileptogenic focus would be stiffer than normal surrounding brain and that therefore SWE may be used to detect this difference.

Case Report

A 7-year-old boy presented with 5-year history of medication-resistant frontal lobe epilepsy. He had two types of seizures: focal seizures with epigastric aura followed by vocal and bilateral motor seizure, and atonic seizures. Both types of seizures occurred on average 10 times per day.

His neurologic examination was normal. Interictal electroencephalography (EEG) recorded epileptiform spikes over the right frontal/anterior temporal region. During a

Accepted January 9, 2014; Early View publication March 1, 2014.
*Department of Neurosurgery, The National Hospital for Neurology and Neurosurgery, London, United Kingdom; †Joint Department of Physics, Institute of Cancer Research, Sutton, Surrey, United Kingdom; ‡Department of Neurophysiology, Great Ormond Street Hospital for Children, London, United Kingdom; §Department of Radiology, Great Ormond Street Hospital for Children, London, United Kingdom; ¶Neurosciences Unit, UCL—Institute of Child Health, London, United Kingdom; and #Department of Neurosurgery, Great Ormond Street Hospital for Children, London, United Kingdom

Address correspondence to Huan Wee Chan, Department of Neurosurgery, The National Hospital for Neurology and Neurosurgery, Queen Square, London WC1N 3BG, U.K. E-mail: chanhuanwee@gmail.com

Wiley Periodicals, Inc.

4-day video-EEG telemetry several stereotypical seizures were captured. The ictal onset was consistently from the right anterior areas (maximal F8 and F10). Interictal spikes were seen over leads C4 and C6, with intermittent slowing on the right frontal region. Four MRI scans, including a 3-T MRI scan, did not demonstrate any lesion. Single photon emission computed tomography (SPECT) showed relative increased tracer uptake in the right cerebral hemisphere, especially the posterior temporal region, not concordant with EEG findings (Fig. 1A). Fluorodeoxyglucose positron emission tomography (FDG-PET) scan revealed a focal area of decreased tracer uptake in the right mid-frontal region and anterior temporal region, concordant with EEG localization (Fig. 1B). Magnetoencephalography (MEG) localized an abnormal area in the right frontal lobe.

Based on the concordant EEG, MEG, and PET, invasive electrode recording was performed in this lesion-negative case. A 64-contact subdural grid (Ad-tech, 8 cm × 8 cm) was placed covering the right frontal region, and two, 6-contact subdural strips (1 cm × 6 cm) were placed over the frontal and temporal poles, respectively (Fig. 1C,D). A two-contact subdural strip was placed against the skull in the posterior region for ground and reference. A depth electrode was placed under neuronavigation and SWE guidance.

Following dural opening and prior to implantation of the grid, both intraoperative ultrasound and SWE were performed using Aixplorer (Supersonic Imagine) scanner equipped with a multifrequency sector transducer (SE12-3) having a bandwidth of 3–12 MHz, with a center frequency of 7.5 MHz. The ultrasound transducer was draped with a

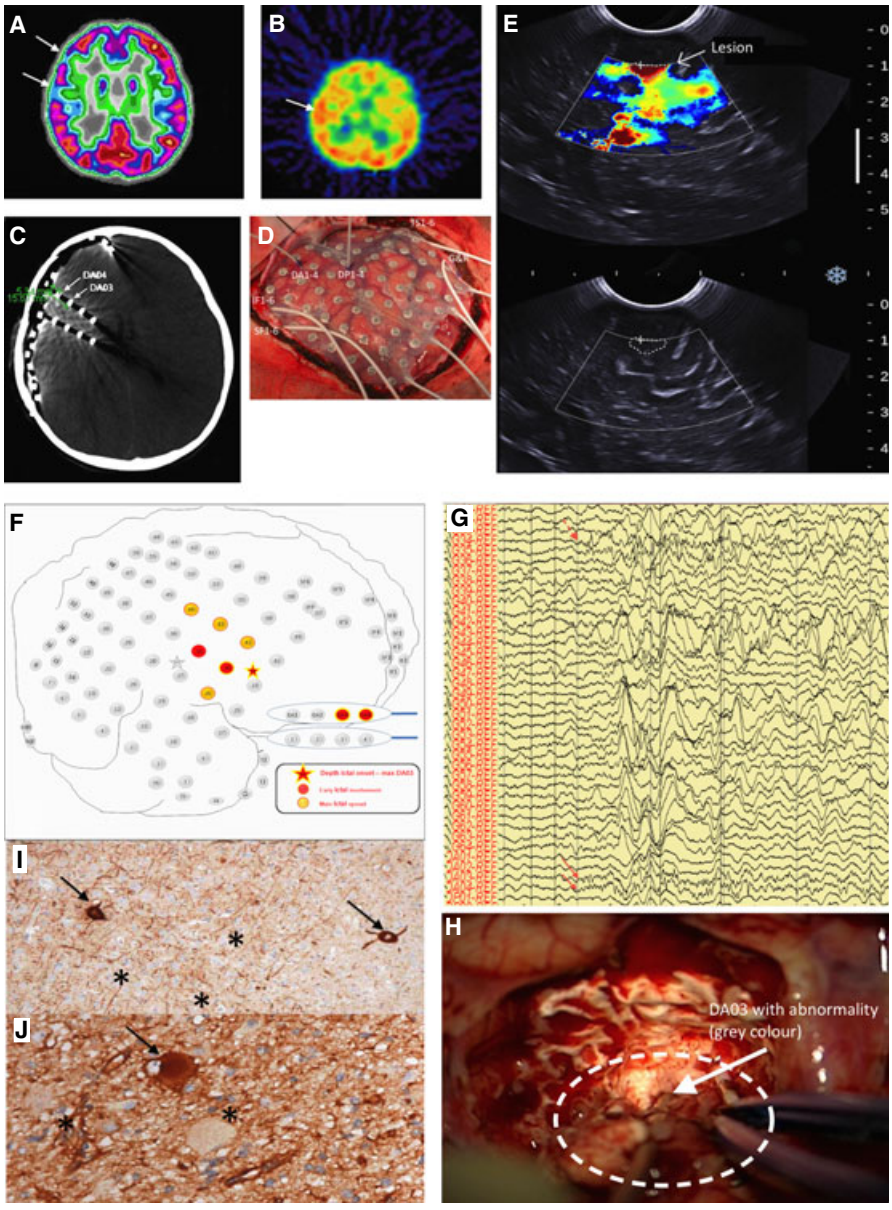

Figure 1.
(**A**) Ictal SPECT showing area of hypermetabolism in the posterior frontal area (arrow). (**B**) FDG-PET showing area of hypometabolism over the right posterior frontal and anterior temporal regions (arrows). (**C**) Postimplantation CT scan and (**D**) intraoperative photograph showing the location of the subdural grid and depth electrodes. DA, anterior depth electrode; DP, posterior depth electrode; SF, superior frontal strip; IF, inferior frontal strip; TS, temporal strip; G&R, ground and reference; 1–64, Subdural grid. (**E**) The display on SuperSonic Aixplorer scanner, where the top and bottom diagrams are elasticity map with SWE and
B-mode ultrasound, respectively. The area of increased stiffness (arrow) was around 1.5 cm from the brain surface. The B-mode image did not show any abnormality. (**F**) Subdural grid and depth electrodes showing ictal onset and spread, with corresponding (**G**) EEG activity starting at DA03 and DA04 (red arrows) with early spread to G34 (dotted red arrow). (**H**) Intraoperative photograph showing the grey abnormally stiff tissue at the depth of DA03 (arrow). Low (**I**) and high magnifications (**J**) of the lesion showing giant neurons (arrow) and balloon cells (asterisks).

sterile transparent plastic sheath, which was filled with sterile acoustic coupling aqueous-based gel. A sweep with high quality B-mode imaging was performed, and no lesion was detected. B-mode ultrasound showed no obvious lesion, but SWE revealed a focal area of increased stiffness approximately 1.5 cm from the brain surface (Fig. 1E). This area had a mean Young's modulus (YM) of 74.7 kPa, compared to the surrounding gray and white matter, which had mean YM of 36.2 and 20.8 kPa, respectively. Because of the SWE finding, a depth electrode was implanted into this region.

During a 6-day period of recording, the patient had 11 diurnal and one nocturnal stereotypical seizures with consistent EEG changes. During his seizures, electrographic onset preceded clinical onset. At onset, low-amplitude fast activity started at DA03 (third contact of the anterior depth electrode 1.5 cm from brain surface), with early involvement of contacts DA04 (fourth contact of the anterior depth electrode 0.5 cm from brain surface) and G34 of subdural grid (Fig. 1F,G). Sometimes the activity started at all three contacts simultaneously. The activity then spread rapidly to contacts G26, G33–35, and G42–44 before involving wider areas.

A resection was planned as shown in the schematic diagram in Figure 1F. This involved resection of the inferior frontal gyrus and frontal operculum along the anterior depth electrode track. A circumferential resection around the depth electrode was performed. At the depth of DA03, the brain tissue appeared gray and felt stiffer than normal brain, which agreed with the SWE findings (Fig. 1H). The resection continued until normal brain was seen; the total volume resected was around 0.5 cc. The lesion was confirmed to be type IIb focal cortical dysplasia (FCD) on histopathologic examination with the presence of dysmorphic giant neurons and balloon cells (Fig. 1I,J).

Postoperatively the patient has remained seizure-free (International League Against Epilepsy [ILAE] class 1) with no focal deficit 6 months following the procedure.

Discussion

MRI-negative focal symptomatic epilepsy constitutes only 16% of patients with focal symptomatic epilepsy with surgical success rate of only 38%.[1] The surgical outcomes depend on the extent of resection of the cortical dysplasia,[2] as Chassoux et al.[3] reported a high seizure freedom rate of 88% in this group where 20% underwent further procedure. Therefore, these patients normally require invasive intracerebral depth electrode recordings to localize the epileptogenic zone. In our case, we performed both intracerebral depth electrodes and subdural grid recordings.

Although high-field 3 T MRI scan can improve detection rates of epileptogenic zones by up to 20%,[4] it is inferior to standard 1.5-T MRI in detecting tissue loss and mesial temporal sclerosis.[5] Our case underwent standard 1.5 T MRI scan first before undergoing 3 T MRI scan, but both scans failed to demonstrate the lesion.

Ictal SPECT can identify areas of increased blood flow following seizure onset, but in our case it failed to identify the epileptic focus.

On the other hand, FDG-PET successfully detected the area of the lesion concordant with EEG findings in our patient. However, due to the poor resolution of FDG-PET, it was not possible to pinpoint the exact area of the lesion.

Subdural grid recordings demonstrate epileptogenic zones in two-dimensional view only without pinpointing the exact location of the lesion.[6] Furthermore, it may be misleading especially if the lesion is at depth. In our case, although the subdural grid improved localization of the epileptogenic zone, it was the depth electrode that pinpointed the exact location of the lesion, which was deep to this area.

Intracerebral depth electrode monitoring is considered invasive, with complication rates for serious morbidity between 0.5% and 5%.[7] This was necessary in our case to localize the epileptic focus and did not cause any complication.

MEG can localize eloquent cortex and epileptogenic onset through magnetic fields produced by electrical activities in the brain. MEG-guided resection in MRI-negative cases resulted in 61.5% achieving Engel class I and II.[8] In our case, of the 50 recording datasets performed, only one localized to the right frontal region. Although the yield of this technique in our patient was low—2%—it was useful in guiding presurgical planning.

Intraoperative B-mode ultrasonography in neurosurgery has been used for real-time diagnosis and surgical guidance since 1980.[9] It was shown to be helpful in defining type IIb FCD in a small series.[10] However, in our case B-mode ultrasonography failed to show the abnormality.

Strain ultrasonography is a technique whereby the soft tissues are subjected to an external force to generate strain within the soft tissues. Selbekk et al.,[11] with the transducer held stationary on the brain surface, used brain pulsation as the external force to generate strain, whereas Chakraborty et al.[12] and Uff et al.[13] used gentle pressure from the transducer on the brain to create strain within the brain and tumor. As the external force used to generate strain is not uniform, it is not possible to calculate the Young's modulus, and thereby quantify the stiffness in soft tissue. The external force used is also subjected to variation between operators; therefore, the quality of strain elastograms (the images generated by strain ultrasonography) is also operator dependent and thus potentially has higher interoperator variability compared with SWE.

SWE estimates the Young's modulus by measuring the shear wave propagation speed in soft tissues, which is generated by highly focused ultrasound beam, known as acoustic radiation force, emitted by the ultrasound transducer. Therefore, SWE does not require external force and thus has less interoperator variability. The Young's modulus is related to shear wave speed by the equation $E \approx 3\rho c^2$, where E is Young's modulus, ρ is soft tissue density, and c

is the shear wave propagation speed. Therefore, SWE is also able to quantify Young's modulus.

Clinically, SWE has been used to characterize different lesions in salivary gland, thyroid, breast, gastrointestinal tract, prostate, and liver.[14] The only SWE evaluation in the brain was performed in trepanated rats, where a three-dimensional brain elasticity map was created with good spatial resolution.[15] Using intraoperative SWE, the dysplastic lesion was successfully outlined as abnormally stiff with a mean Young's modulus of 74.7 kPa, which was much higher than in normal brain. This abnormal area was confirmed as type IIb FCD on histopathology. Therefore, our case demonstrated, for the first time, the use of SWE intraoperatively to localize epileptogenic focus absent on both 3 T MRI and B-mode ultrasound.

Shear wave propagation speed is influenced by anisotropy of the soft tissue. For example, in skeletal muscles, shear wave propagates faster along the muscle fibers than across them.[16] Similarly, Macé et al.[15] demonstrated anisotropy in white matter, that is, there was a significant difference in the shear wave speeds in the same tissue on different scan planes, and postulated that the orientation of the axonal fibers is responsible for the anisotropy. Therefore, as the area of increased stiffness at about 3-cm depth corresponds to white matter, it is possible that the white matter tracts run horizontally in that region. On the B-mode, the speckle pattern in that region, which has the appearance of horizontal lines, is also suggestive of a horizontal orientation of the white matter tracts. In addition, the depth electrode did not pick up any electrical disturbance in that area. Therefore, SWE should be used as an intraoperative adjunct and interpreted with electrophysiologic studies.

This case report illustrates how we converted a nonlesional epilepsy case into a lesional case. The MRI and ictal SPECT did not identify the lesion. The FDG-PET detected the lesion, and therefore helped guide the craniotomy and electrode placements, but was not sufficiently precise to guide resection. By exploiting the abnormal stiffness of this lesion, SWE successfully delineated the lesion, which was later confirmed by electrophysiologic and histopathologic findings. Although B-mode ultrasound did not show the lesion, it demonstrated the anatomic details that were not present on SWE. Therefore, by superimposing the two images, which could be configured easily with this scanner, we could pinpoint the lesion with reasonable certainty. This case report has demonstrated that SWE can detect MRI-negative and ultrasound-negative lesion. Therefore, in the future, SWE with B-mode ultrasound should be considered in all patients with nonlesional epilepsy.

SWE can quantify stiffness and does not require deformation of soft tissue by external force. Therefore, SWE can inform the neurosurgeon regarding the consistency of the lesion prior to resection, thereby facilitating safer surgery. Second, because B-mode ultrasound sometimes does not show the lesion clearly, and in this case not at all, SWE allows the neurosurgeon to visualize the lesion and its boundaries. Third, as it does not require external force, it has less interoperator variability, and is also more attractive for intraoperative use, especially in neurosurgery where unnecessary manipulation of the brain is not preferred.

Disclosure

This study has ethical approval from the National Research Ethics Service (NRES) Committee London – Queen Square Research Ethics Committee (Ref: 08/H0716/92). None of the authors has any conflict of interest to disclose. We confirm that we have read the Journal's position on issues involved in ethical publication and affirm that this report is consistent with those guidelines.

References

1. Bien CG, Szinay M, Wagner J, et al. Characteristics and surgical outcomes of patients with refractory magnetic resonance imaging-negative epilepsies. *Arch Neurol* 2009;66:1491–1499.
2. Cohen-Gadol AA, Ozduman K, Bronen RA, et al. Long-term outcome after epilepsy surgery for focal cortical dysplasia. *J Neurosurg* 2009;101:55–65.
3. Chassoux F, Landré E, Mellerio C, et al. Type II focal cortical dysplasia: electroclinical phenotype and surgical outcome related to imaging. *Epilepsia* 2012;53:349–358.
4. Strandberg M, Larsson EM, Backman S, et al. Pre-surgical epilepsy evaluation using 3T MRI. Do surface coils provide additional information? *Epileptic Disord* 2008;10:83–92.
5. Zijlmans M, de Kort GA, Witkamp TD, et al. 3 T versus 1.5 T phased-array MRI in the presurgical work-up of patients with partial epilepsy of uncertain focus. *J Magn Reson Imaging* 2009;30:256–262.
6. Lüders H, Awad I, Burgess R, et al. Subdural electrodes in the presurgical evaluation for surgery of epilepsy. *Epilepsy Res Suppl* 1992;5:147–156.
7. Ross DA, Brunberg JA, Drury I, et al. Intracerebral depth electrode monitoring in partial epilepsy: the morbidity and efficacy of placement using magnetic resonance image-guided stereotactic surgery. *Neurosurgery* 1996;39:327–333.
8. Wu XT, Rampp S, Buchfelder M, et al. Interictal magnetoencephalography used in magnetic resonance imaging-negative patients with epilepsy. *Acta Neurol Scand* 2013;127:274–280.
9. Wang Y-D, Wang Y, Mao Y, et al. Intraoperative ultrasound assistance in the resection of small, deep-seated, or ill-defined intracerebral lesions. *Chin Med J (Engl)* 2011;124:3302–3308.
10. Miller D, Knake S, Menzler K, et al. Intraoperative ultrasound in malformations of cortical development. *Ultraschall Med* 2011;32 (Suppl. 2):E69–E74.
11. Selbekk T, Brekken R, Indergaard M, et al. Comparison of contrast in brightness mode and strain ultrasonography of glial brain tumours. *BMC Med Imaging* 2012;12:11.
12. Chakraborty A, Berry G, Bamber J, et al. Intra-operative ultrasound elastography and registered magnetic resonance imaging of brain tumours: a feasibility study. *Ultrasound* 2006;14:43–49.
13. Uff CE, Garcia L, Fromageau J, et al. Real-time ultrasound elastography in neurosurgery. Ultrasonics Symposium IUS 2009 IEEE International 2009:467–470.
14. Cosgrove D, Piscaglia F, Bamber J, et al. EFSUMB guidelines and recommendations on the clinical use of elastography. Part 2: clinical applications. *Ultraschall Med* 2013;34:238–253.
15. Macé E, Cohen I, Montaldo G, et al. In vivo mapping of brain elasticity in small animals using shear wave imaging. *IEEE Trans Med Imaging* 2011;30:550–558.
16. Gennisson J-L, Deffieux T, Macé E, et al. Viscoelastic and anisotropic mechanical properties of in vivo muscle tissue assessed by supersonic shear imaging. *Ultrasound Med Biol* 2010;36:789–801.